

FR8502808

Doc Saclay

2  
23. International meeting on nuclear physics  
Bormio (Italy) 21-26 Jan 1985  
CEA-CONF--7807

Rapport DPh-N/Saclay n°2233

02/1985

Nucleus-nucleus interactions in the transition energy regime

Claude VOLANT

Service de Physique Nucléaire-Basse Energie,  
CEN Saclay, F-91191 Gif-sur-Yvette cedex, France

## NUCLEUS-NUCLEUS INTERACTIONS IN THE TRANSITION ENERGY REGIME

C. VOLANT

Service de Physique Nucléaire - Basse Energie,  
CEN Saclay, 91191 Gif-sur-Yvette Cedex, France

It has been predicted many years ago that the heavy ion physics between 10 to 100 MeV/u must reveal a lot of exciting features. More precisely, how could proceed the transition from a reaction mechanism dominated by the mean nuclear field to another one governed by the nucleon-nucleon interaction. Nowadays, heavy ion beams just begin to be available in this energy domain and recent experimental results obtained by our group will be reported here.

One can expect to observe such a transition in the degree of collectivity of the nucleus-nucleus interactions which must decrease in this energy region. One possibility is to look to the largest cooperant process which is the fusion of the two nuclei and to see how complete is the relaxation of the degrees of freedom.

There are at least two ways for studying such large interactions in nucleus-nucleus collisions. One of them is to detect directly the evaporation residues from the composite system ; this method seems the most straightforward but the experimental results might not be always easy to interpret since we have to deal with measurements of single events when a lot of fragments are emitted which can be mixed with the evaporation residues resulting from very long evaporation chains. Another class of experiments and that is the domain in which our group has been working since a few years, is to use the method of angular correlations between fission fragments <sup>1</sup>).

In that method, by making a few assumptions, one can relate the folding angle distribution of the fission fragments to the distribution of the linear momenta transferred to the target by the projectile. Furthermore by improving this method in adding measurements of the velocities and energies of both fragments <sup>2</sup>) one accesses to more detailed informations on the mechanism such as the recoil velocities, the mass distributions and the energy deposited during the interactions.

The aim of the experiments presented here was to make a survey on the role of the various experimental parameters. In that respect three targets have been studied :  $^{232}\text{Th}$ ,  $^{197}\text{Au}$  and  $^{165}\text{Ho}$  and different projectiles and bombarding energies have been used :

-  $\alpha$ -particles at 70 and 250 MeV/u at Saturne by the following collaboration : G. Klotz, H. Oeschler, E. Kankeleit (IFK Darmstadt), Y. Cassagnou, M. Conjeaud, R. Dayras, S. Harar, R. Legrain, M.S. Nguyen, E.C. Pollacco, C. Volant (DPHN/BE Saclay).

-  $^{14}\text{N}$  projectiles at 60 MeV/u and  $^{40}\text{Ar}$  beam from 31 to 44 MeV/u at Ganil with the following participants : Y. Cassagnou, M. Conjeaud, R. Dayras, S. Harar, R. Legrain, M. Mostefaï, E.C. Pollacco, C. Volant (DPHN/BE Saclay), H. Oeschler (IFK Darmstadt), F. Saint-Laurent (Ganil).

A few years ago, we proposed a classification of the reaction mechanisms in three regimes <sup>3)</sup> versus the incident energy based on the variation of the average linear momentum transferred by p, d and  $\alpha$ -particles on fissile targets (fig. 1) :

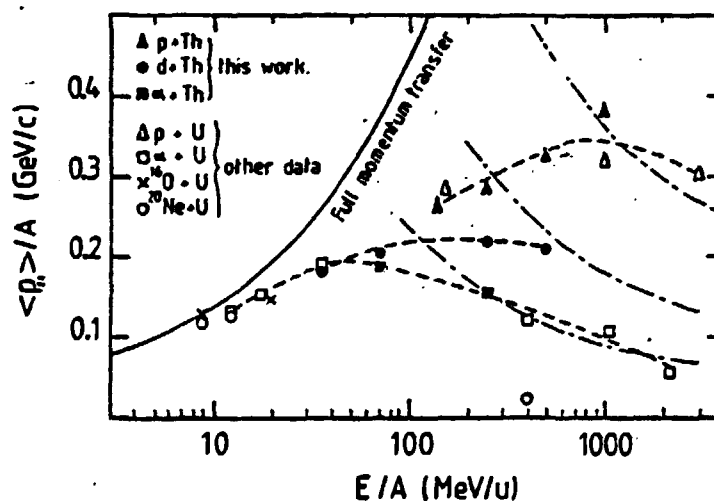


Fig. 1 - Average momentum transfer per projectile nucleon versus the bombarding energy per nucleon. Dashed curves are to guide the eye, dotted-dashed curves are calculated following equation(1) with  $E^* = 160$  MeV.

- 1) Below 10 MeV/u the full linear momentum transfer (FMT) is the most probable.
- 2) Between 10 and 70 MeV/u, the FMT is no more reached but a scaling with the projectile mass is observed showing that still a collective effect persists.
- 3) Above 70 MeV/u, the scaling is lost and a decrease of  $\langle P_{\parallel} \rangle / A$  is observed which can be interpreted as a limit in the mean excitation energy  $E^*$  beyond which the system decays in other channels than fission. The empirical relation derived by Porile<sup>4)</sup> from intranuclear cascade calculations (INC) :  $E^* / E_{CN} = 0,75(P_{\parallel} / P_{CN})$  (1) where  $P_{CN}$  and  $E_{CN}$  are the momentum and excitation energy the compound nucleus would have, fits quite well the high energy data in fig. 1 by choosing  $E^* = 160$  MeV.

Alpha induced fission

The influence of the targets has been studied recently <sup>5)</sup> and angular correlations on Th, Au and Ho translated in a linear momentum scale are shown in fig. 2 for two  $\alpha$ -particle bombarding energies : 70 and 250 MeV/u.

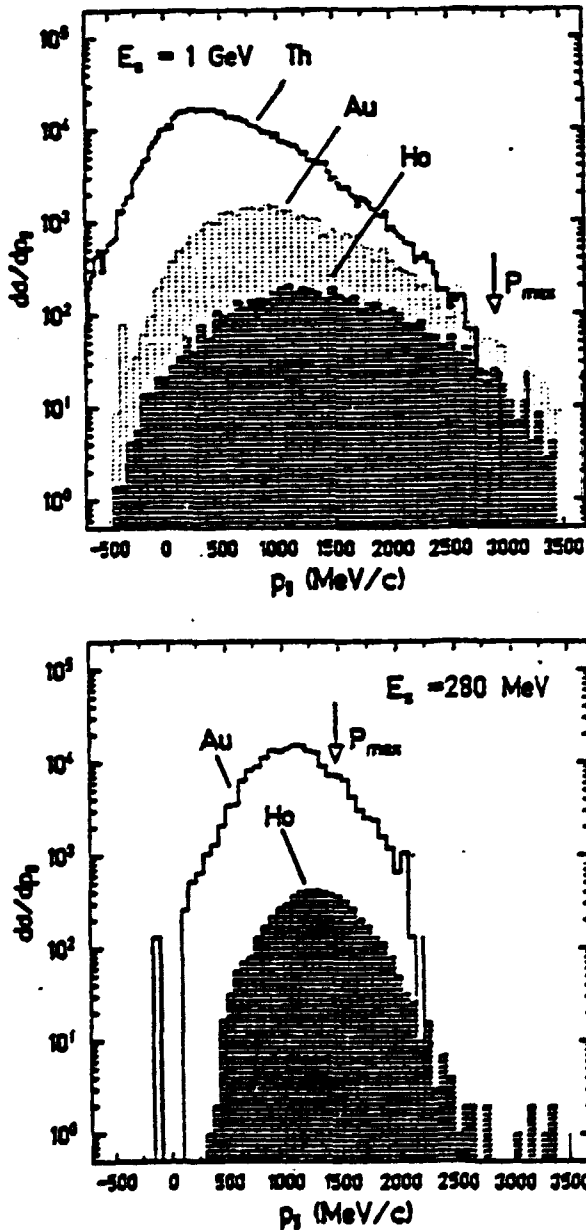


Fig. 2 - Linear momentum distributions obtained from fission fragment angular correlations when bombarding Th, Au and Ho targets by  $\alpha$ -particles at 1 GeV and 280 MeV incident energies. Arrows indicate the full momentum transfer.

A selectivity in P distributions is observed for the less fissile Au and Ho targets whereas a broad distribution is observed for the Th target ranging from sequential fission to more violent collisions.

This selectivity can be interpreted as a manifestation of the fission barrier differences for the targets but it also evidences that on a fissile target we effectively measure a momentum distribution and that the choice of targets acts as a filter on the momentum space, selection which is paid by a drastic decrease of the cross sections. A few remarks can be added :

- Masses and velocities of the fragments have been measured and they present the same characteristics as observed at low energies <sup>6,7)</sup> showing we are dealing with normal fission.

- On the Ho target at 70 MeV/u almost the FMT is reached indicating that at twice the Fermi velocity the  $\alpha$ -particle can be stopped in the target.

- At both energies the mean linear momentum transfer remains constant but is larger for lower target masses.

Hence, the saturation effect observed on Th (fig. 1) in this energy region exists whatever the target is, but it depends of its mass.

Table 1

Comparison of mean relative momentum transfers  $P_{ii} / P_i$  and fission fragment masses  $A$  measured in fission induced by  $\alpha$ -particles and protons at 1 GeV incident energy. The mean excitation energies  $E^*$  have been calculated using equation (1).

	alpha $P_\alpha = 2,91$ GeV/c			proton $P_p = 1,69$ GeV/c		
Targets	<sup>232</sup> <sub>90</sub> Th	<sup>197</sup> <sub>79</sub> Au	<sup>165</sup> <sub>67</sub> Ho	<sup>232</sup> <sub>90</sub> Th	<sup>197</sup> <sub>79</sub> Au	<sup>165</sup> <sub>67</sub> Ho
$P_{ii} / P_i$	0,24	0,34	0,45	0,26	0,32	0,47
$A$ a.m.u	108	86	64	108	84	?
$E^*$ MeV	179	253	327	194	239	352

On table 1 are compared the fission properties observed on the same targets bombarded by  $\alpha$ -particles and protons <sup>8)</sup> of 1 GeV. The measured mean values of  $P_{ii} / P_i$  and masses are identical in both experiments. The mass measurements confirm that the excitation energies calculated by formula (1) are the same in both cases and quite in agreement with the value of 160 MeV quoted in fig. 1 for the Th target. One can however notice that we are dealing with mean values and that this apparent limitation translates the selectivity due to the target properties.

These measurements serve to illustrate what is the behaviour in the energy domain where the nucleon-nucleon interaction is expected to be dominant.

#### <sup>14</sup>N induced fission

To come back to the transition region and before to comment on the  $\alpha$ -particle 70 MeV/u data let us turn to recent results obtained with the <sup>14</sup>N beam of 60 MeV/u for the same targets. Here again a nice selectivity is observed (fig. 3) in the linear momentum distribution which also results in a strong decrease of the cross-sections for the lightest targets. For comparison are also shown on fig. 3 the 60 MeV/u <sup>12</sup>C data obtained at CERN <sup>9)</sup> for only two targets and the general trend is the same : on Th, besides the sequential fission peak, a shoulder is seen at high momentum whereas a single bump exists for Au. Furthermore the <sup>12</sup>C, despite its known structure, does not appear to be so fragile since it seems even more efficient in a relative momentum transfer basis ; however we can notice that in absolute value the scaling observed in fig. 1 is still reasonable valid for these two ions.

On fig. 4 are shown preliminary results on mass measurements for the three studied systems versus the relative transferred linear momentum : smaller are the masses, larger are the momentum transfers illustrating well an increase of the violence of the collision ; the dashed lines in fig. 4

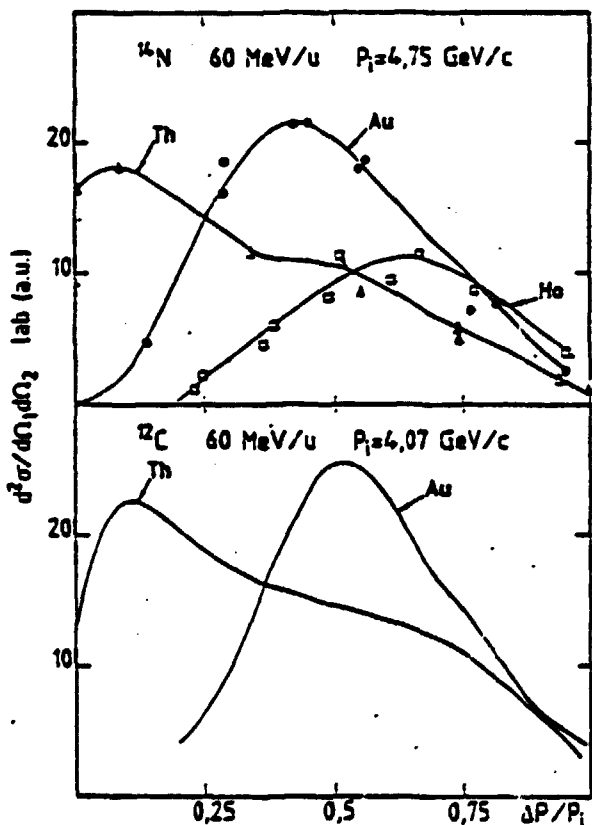


Fig. 3 - Linear momentum distributions obtained from in-plane fission fragment angular correlations when bombarding Th, Au and Ho targets by 60 MeV/u  $^{14}\text{N}$  projectiles (upper part). Schematic drawing of the same data for 60 MeV/u  $^{12}\text{C}$  projectiles <sup>9)</sup> (lower part).  $\Delta P/P_1$  is the ratio of the transferred linear momentum  $\Delta P$  to the incident one  $P_1$ .

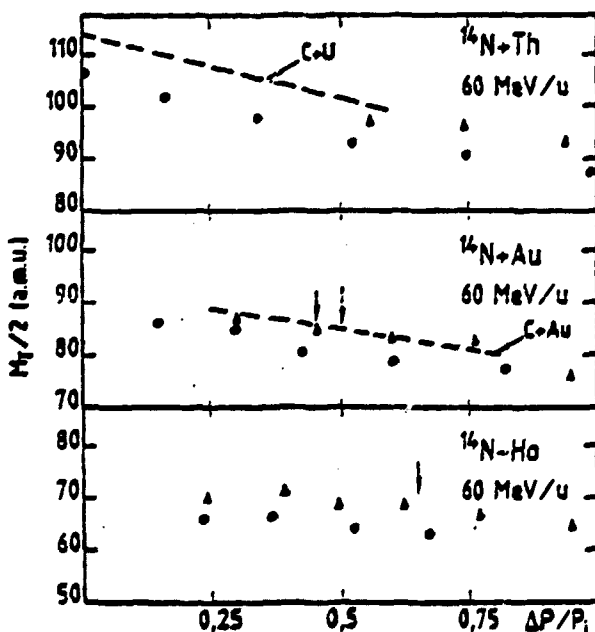


Fig. 4 - Preliminary measurements of the mean half total masses of the fission fragments versus the relative transferred linear momentum for 60 MeV/u  $^{14}\text{N}$  projectiles on Th, Au and Ho. Triangles and points indicate two different sets of measurements and illustrate the uncertainties. Dashed lines are results from 60 MeV/u  $^{12}\text{C}$  experiments <sup>10)</sup>. Arrows indicate the maximum of the correlations.

represent the measurements for the 60 MeV/u  $^{12}\text{C}$  ions <sup>10)</sup> which agree quite well for the gold target if the mass differences between  $^{14}\text{N}$  and  $^{12}\text{C}$  can be neglected in respect to the error bars not yet evaluated and a larger discrepancy for U could be accounted for the target mass differences.

Table 2

Comparison of the experimental fission masses for 70 MeV/u  $\alpha$ -particles and 60 MeV/u  $^{14}\text{N}$  projectiles on Au and Ho targets with calculations using equation (1) INC and the hypothesis of a massive transfer M.T.  $P/P_i$  is the relative momentum transfer at the maximum of the angular correlations.

Targets	$\alpha$ 70 MeV/u $P_i = 1,47$ GeV/c				$^{14}\text{N}$ 60 MeV/u $P_i = 4,75$ GeV/c			
	INC a.m.u	M.T a.m.u	Exp a.m.u	$P/P_i$	INC a.m.u	M.T a.m.u	Exp a.m.u	$P/P_i$
Au	95	92	93	0,73	93	85	85	0,45
Ho	77	75	74	0,82	74	65	68	0,65

$$\text{Massive transfer M.T. } \frac{E^*}{E_{CN}} = \frac{A_T + A_p}{A_T + m} \cdot \frac{P_{//}}{P_i}$$

$A_T$  and  $A_p$  target and projectile masses

$$m \text{ transferred mass } m = \frac{P_{//}}{P_i} \cdot A_p$$

On table 2, evaluations of the masses for Au and Ho targets measured at the maximum of the correlations for 70 MeV/u  $\alpha$ -particles and 60 MeV/u  $^{14}\text{N}$  are done following two crude alternatives : one taken from the already mentioned Porile's estimate and the other using the naive picture of a massive transfer of a part of the projectile to the target, the remaining ejectile carrying away the missing momentum. The masses are then deduced from the calculated excitation energies with the assumption that the average energy removed by nucleon emitted is 12 MeV. The massive transfer works quite well for the  $^{14}\text{N}$  case but both calculations agree with the  $\alpha$ 's data although one cannot expect the intranuclear cascade calculations to be valid at a so low velocity. In fact both formulae used in table 2 are not so different for light projectiles and they diverge only significantly for heavy projectiles. At this point one can remember that in the 70 MeV/u  $\alpha$ 's data there is still persistence of collective aspects since we do observe the almost full momentum transfer on the Ho target and evidences for the importance of massive transfers have been obtained in a triple coincidence experiment between fission fragments and ejectiles (fig. 5). The maxima of the angular correlations for each ejectile follow the trend expected for the transfer to the target of the remaining part of the projectile.

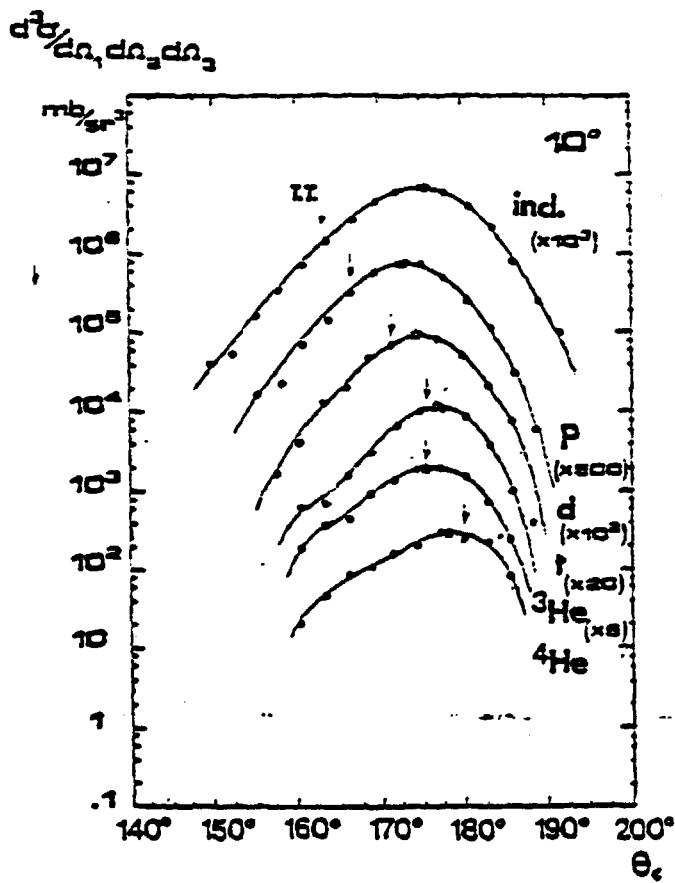


Fig. 5 - Angular correlations  $\alpha + {}^{232}\text{Th}$  at 70 MeV/u. The curve labelled incl is for fission fragment coincidences only. Curves labelled with p, d, t,  ${}^3\text{He}$  and  ${}^4\text{He}$  are angular correlations gated by the corresponding ejectiles detected at  $10^\circ$  lab. Points are experimental results, lines are to guide the eye. Arrows indicate the expected location of the full momentum transfer of the remaining part of the projectile.

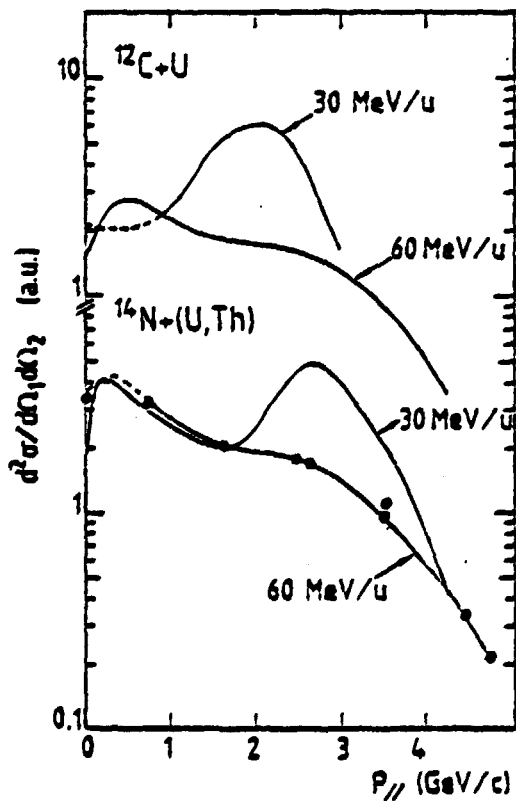


Fig. 6 - Schematic drawing of the linear momentum distributions deduced from angular correlations between fission fragments in  ${}^{12}\text{C}$  induced fission at 30 and 60 MeV/u (ref. 9)) and 30 MeV/u  ${}^{14}\text{N}$  on U (ref. 11)). Points with a curve drawn to guide the eye are present results for the  ${}^{14}\text{N} + {}^{232}\text{Th}$  system at 60 MeV/u.



To illustrate the bombarding energy influence on the angular correlation pattern, we compare  $^{12}\text{C}$  and  $^{14}\text{N}$  results at 30 MeV/u (refs.<sup>9,11</sup>) and 60 MeV/u on fissile targets in fig. 6.

At 30 MeV/u, in both cases, a bump is clearly seen at  $\sim 2$  GeV/c and 2,6 GeV/c with  $^{12}\text{C}$  and  $^{14}\text{N}$  respectively, at 60 MeV/u a shoulder still remains at the same place despite the increase of the incident momentum, only the cross section for this violent process is lowered ; this aspect will be confirmed in the next section devoted to results obtained with Ar projectiles.

$^{40}\text{Ar}$  induced fission

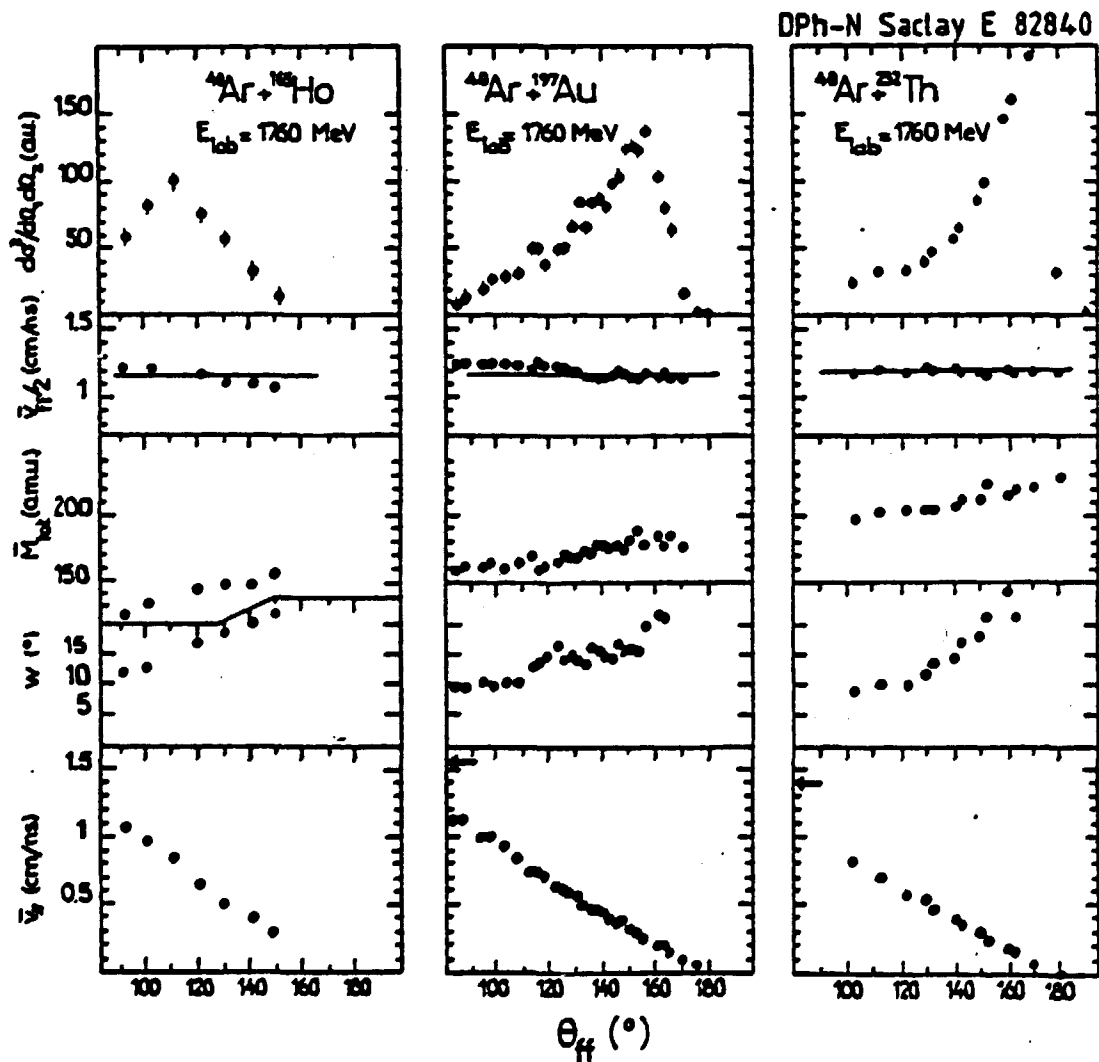


Fig. 7 - Results for  $^{40}\text{Ar} + ^{165}\text{Ho}$  (left part),  $^{40}\text{Ar} + ^{197}\text{Au}$  (middle part) and  $^{40}\text{Ar} + ^{232}\text{Th}$  (right part). a) in-plane angular correlation between fission fragments. b) average velocities of the fission fragments in the recoil fissioning nucleus frame. The solid lines are from Viola systematics. c) mean total mass of the fission fragments. The solid lines are results from calculations in the framework of a massive transfer mechanism. d) half width at the half maximum of the recoil angle distributions. e) mean longitudinal velocity of recoil fissioning nuclei. The arrows indicate the recoil velocities for full momentum transfer.

On fig. 7 are displayed the data obtained with a 44 MeV/u  $^{40}\text{Ar}$  beam on the three targets  $^{2,12}$ ). Here again, a selectivity can be seen since the angular correlations are peaked (fig. 7a) around 7 %, 15 % and 35 % of the beam momentum for Th, Au and Ho targets respectively. A full discussion of this figure is given elsewhere  $^2$ ) and one can stress here a few points :

- The relative velocities of the fission fragments follow the Viola's systematics (full lines in fig. 7b) indicating we are dealing with normal fission.

- The naive interpretation of a massive transfer mechanism reproduces quite well the mass distributions (full lines in fig. 7c).

- We attached significance to the events corresponding at small folding angles since the measured masses and velocities show a continuous trend on the full angular range and we stressed that excitation energies up to 900 MeV have been reached corresponding to momentum transfers of around 7 GeV/c.

The shapes of these angular correlations at 44 MeV/u confirmed by similar measurements  $^{13}$ ) were at that time quite puzzling when compared to lower energy data  $^{14}$ ) as shown in fig. 8 where clearly a bump is seen around 7 GeV/c which is absent in our data although we claimed that the relative rare events seen at large momentum transfers had the same nature.

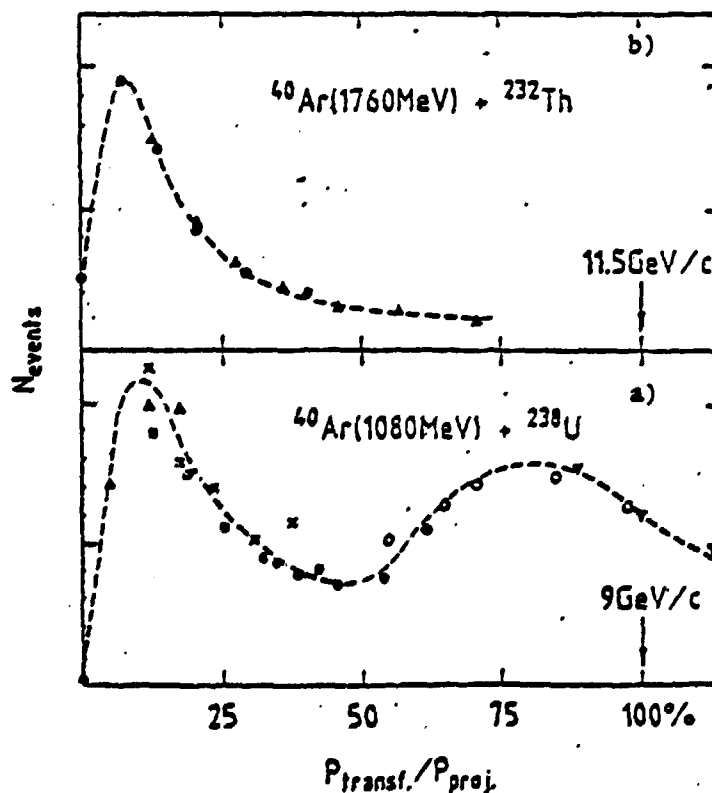


Fig. 8 - Comparison of fission fragments angular correlations for the system  $^{40}\text{Ar} + ^{232}\text{Th}$  at 44 MeV/u and  $^{40}\text{Ar} + ^{238}\text{U}$  at 27 MeV/u (ref.  $^{14}$ )).

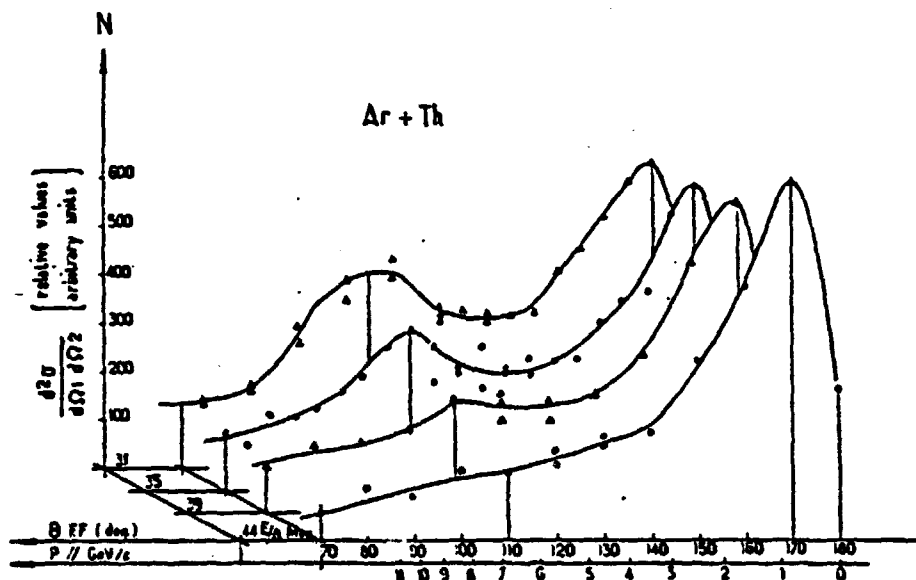


Fig. 9 - In-plane angular correlations of fission fragments for the system  $^{40}\text{Ar} + ^{232}\text{Th}$  at 31, 35, 39 and 44 MeV/u. Curves are drawn to guide the eye. The linear momentum scale  $P_{//}$  is for 44 MeV/u. The bars for each energy correspond to  $\theta_{ff} = 170^\circ$  and  $110^\circ$  (about 0.8 and 7 GeV/c respectively).

In order to see how strong was this transition we measured recently an excitation function for these angular correlations from 31 to 44 MeV/u which is shown in fig. 9. One sees that, in addition to the sequential fission bump which remains about constant, the high momentum bump is vanishing slowly with the bombarding energies staying nevertheless at the same linear momentum around 7 GeV/c. The continuity of this phenomena, whose cross section is decreasing by about of factor of 2 in the studied range, can be illustrated by preliminary mass measurements shown in fig. 10 where are plotted the total masses of both fragments for the regions around the two peaks versus the incident energies. The masses for low transfers remain about constant as expected for peripheral reactions and they are decreasing for the 7 GeV/c region with the increase of the incident energy showing that these central collisions are more and more violent. This can also be reproduced by using the massive transfer as illustrated by the solid lines in fig. 10.

In fig. 11, are shown rough estimations of the integrated cross-sections for both phenomenae versus the incident energies ; despite very large uncertainties essentially due to the assumptions used in the integration, the relative behaviour in respect to the bombarding energy should be less affected. For comparison have been added evaluations of the reaction cross sections  $\sigma_R$  using optical model parameters determined in this energy region<sup>15</sup>). It can be seen that, whereas the peripheral part remains con-

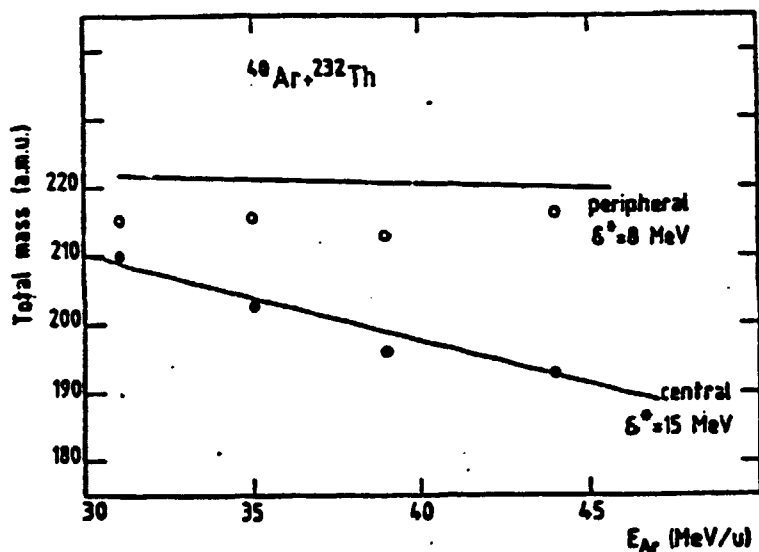


Fig. 10 - Preliminary measurements of the total mass of the fission fragments versus the bombarding energy for the peripheral and "central" ( $\sim 7$  GeV/c) part of the angular correlations of fig. 9. Curves are results of calculations using the massive transfer hypothesis with the average energy  $\epsilon^*$  removed by nucleon evaporated indicated in the figure.

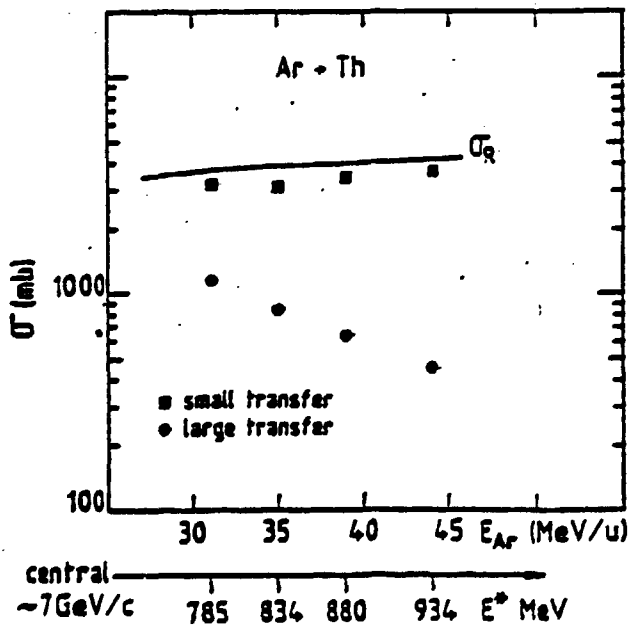


Fig. 11 - Estimated cross sections for the peripheral (rectangles) and central part (black points) of the angular correlations of fig. 9 versus the bombarding energy. Absolute scales could be quite unaccurate and strongly dependent of the integration procedure (a  $1/\sin \theta$  distribution in the center of mass has been assumed for both components). The curve labelled  $\sigma_R$  is the reaction cross section calculated using parameters from <sup>15</sup>). Scale is also given for the estimated excitation energies for central collisions.

constant, the central part decreases almost exponentially with the bombarding energy. This fall-off would be of the same type versus the estimated excitation energies (lower scale in fig. 11) which are very high since they approach 1 GeV, corresponding to temperatures around 5 to 6 MeV.

The data obtained by the angular correlation method on fissile targets permit us to have an overlook on the bulk of the interactions of the projectile since almost all reactions are leading to fission and a rather large part of the cross-section corresponds to large interpenetration of the two ions. Nevertheless limits in inelasticity are observed which are still to be understood. The most probable linear momentum transfer, apart from the "trivial" sequential fission, seems to saturate and indeed present and previous data support the suggestions <sup>16)</sup> of a limit per incident nucleon of around 180 MeV/c which could be interpreted as a threshold were the heated nucleons have large probability to escape. Another observation can be done on the probability of this limiting transfer, for which present data show a decrease with the incident energy which could be due to the effect of the excitation energy increase in the composite system. Other channels than fission could open such as multifragmentation or simply too large evaporation chains leading to non-fissioning nuclei ; more exotic phenomenae could also exhaust a part of the reaction cross section.

A last remark can be done on the target selectivity as schematically shown in fig. 12 for a part of the present data.

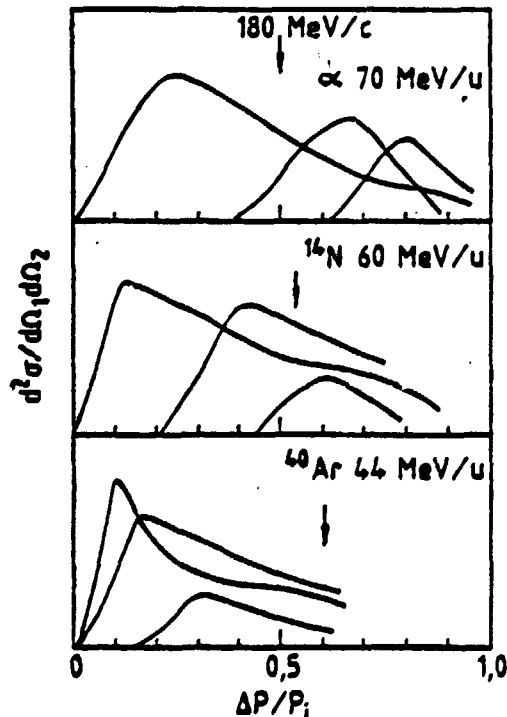


Fig. 12 - Schematic drawing of the angular correlation between fission fragments for a part of the present data. Arrows indicate the location of a linear momentum of 180 MeV/c per incident nucleon.

For the  $\alpha$ 's data it is seen that by no means the magic 180 MeV/c is universal since for the Ho target almost twice this value can be observed ; this effectively occurs with very low cross-sections but it shows that one has an experimental filter, to be paid by beam time, to study very violent collisions. The  $^{14}\text{N}$ 's data look like intermediate since the Ho target selects higher values than 180 MeV/c and Au lower ones. The Ar's data show that this selectivity does not act on the large momentum part but probably excitation energy and angular momentum limits for fission of Au and Ho are already reached with low relative linear momentum transfer by this heavy projectile. However this does not exclude the existence of significant component of large momenta although no clear bumps are visible at 44 MeV/u.

#### References

- 1) T.Sikkeland et al., Phys. Rev. 125 (1962) 1350
- 2) E.C. Pollacco et al., Phys. Lett. 146 B (1984) 29
- 3) F. Saint-Laurent et al., Phys. Lett. 110 B (1982) 372  
F. Saint-Laurent et al., Nucl. Phys. A 482 (1984) 307
- 4) N.T. Porile, Phys. Rev. 120 (1960) 572
- 5) G. Klotz et al, in preparation
- 6) J.R. Nix Nucl, Phys. A 130 (1969) 241
- 7) V.E. Viola, Nucl. Data Sect A 1 (1966) 391
- 8) L.N. Andronenko et al, Z. Phys. A 318 (1984) 97 and references therein
- 9) J. Galin et al Phys. Rev. Lett. 48 (1982) 1787
- 10) M.F. Rivet et al., Bormio 1983
- 11) M.B. Tsang et al., Phys. Lett. 134 B (1984) 169
- 12) Y. Cassagnou et al., INS Riken International Symposium on heavy ion physics, Mont-Fuji August 27-31, 1984
- 13) S. Leray et al., Nucl. Phys. A 425 (1984) 345
- 14) D. Jacquet et al., Phys. Rev. Lett. 53 (1984) 2226 ;  
M.F. Rivet and B. Borderie, Tsukuba International Symposium on heavy ion fusion reactions, September 3-5, 1984
- 15) P. Roussel, private communication
- 16) J.L. Laville et al, Phys. Lett. 138 B (1984) 35